10th CIRP Conference on Photonic Technologies [LANE 2018]

Coaxial laser triangulation for height monitoring in laser metal deposition

Simone Donadello[a,*], Maurizio Motta[a], Ali Gökhan Demir[a], Barbara Previtali[a]

aDepartment of Mechanical Engineering, Politecnico di Milano, Via La Masa 1, 20156 Milan, Italy

* Corresponding author. Tel.: +39-02-2399-8593 ; fax: +39-02-2399-8585. *E-mail address:* simone.donadello@polimi.it

Abstract

The control of the height parameter plays a crucial role in the laser metal deposition (LMD) process. A mismatch between the deposition height increment and the process growth rate can generate geometrical inaccuracies as well as collisions. The paper presents a method based on triangulation for monitoring in-line the height on a LMD system composed of a coaxial deposition head, an anthropomorphic robot and a fiber laser. The measurement device is implemented within the deposition head, with a probe laser beam that is launched coaxially through the nozzle and focused directly on the melt pool at different positions depending on the standoff distance. The position of the probe spot is acquired through a coaxial camera and converted in relative height values. The system is demonstrated for the distance measurement over a range of some millimeters during the deposition of AISI 316L stainless steel. This method allows for high flexibility being independent on the deposition direction.

1. Introduction

The laser metal deposition (LMD) process consists in melting metallic micrometric powder by means of an energy source, specifically a laser beam. This technology finds several applications in many technological fields such as additive manufacturing [1]. Typically, the powder is carried by an inert gas and sprayed by a nozzle in a coaxial way: in its focal point the conical powder flow overlaps the laser beam which passes through the middle of the nozzle, hence generating a melt material pool on a substrate. The subsequent solidification creates a solid layer of deposited material and consequently, layer by layer, a structure can be built up.

The standoff distance (SOD), i.e. the distance between the nozzle tip and the deposition area, is a key factor in the LMD process in order to have a regular and controlled deposition [2, 3]. An ideal SOD allows for an optimal overlapping between the focused laser beam and the conical powder flow: a variation of this parameter brings to changes in the deposition properties. In fact, if the SOD increases the powder focalizes above the substrate and the subsequent layer might not be deposited efficiently; on the contrary, if the SOD

decreases the powder hits the structure before its focal point and the interaction with the laser beam may be altered; a big SOD decrement can lead even to collisions or molten particles aggregated inside the inner channels of the nozzle.

In multi-layer depositions SOD variations can arise in the case of discrepancy between the expected and actual heights of the deposited layers, hence controlling the deposition height parameter becomes important in terms of the process quality [4, 5]. Post-process approaches for the SOD optimization are often employed. However, methods for a continuous and real-time monitoring would be preferable for an active and flexible control of the deposition process. In general, optical methods can be used for precise and fast distance measurements. Several studies employed standard laser displacement sensors or scanners for monitoring the additive process, with measurement units attached off-axis to the deposition device [6, 7, 8, 9, 10]. Other works reported the use of digital image recognition methods for monitoring the deposition growth [11, 12]. However, such approaches typically need bulky and complex systems that limit their flexibility. Another limitation of such kinds of off-axis measurements can be their intrinsic dependence on the

deposition direction, particularly in the presence of complex 3D geometries which may introduce blind zones and shadowing effects.

The current work presents a novel and non-intrusive setup for the in-situ height monitoring applied on a deposition head controlled by means of a robot. The measurement principle is based on optical triangulation implemented in a quasi-coaxial way, which allows for high flexibility in terms of deposition direction and strategy. The monitoring device results to be simple, cheap and compact, and after its calibration it has been demonstrated during the LMD process. In future this might be employed for the in-line optimization of the deposition parameters according to the effective deposition growth.

Nomenclature

h_{robot}	height increment of the robot at each layer
h_{layer}	effective height of a single deposited layer
H_{robot}	cumulative height programmed to the robot
H_{tot}	effective total height of the deposited structure
SOD	standoff distance between the nozzle tip and the deposition area
z_t	vertical distance between the optical focal point and the probed target surface
z_0	initial distance between the optical focal point and the substrate at the reference SOD
y_1	position of the probe laser spot in the horizontal plane
y_2	coordinate of the probe spot imaged on the camera

2. System design and implementation

2.1. LMD setup

The LMD setup includes a 1070 nm active fiber laser source (IPG YLS-3000) with a maximum power of 3 kW and operated at 400 W. The optical radiation is delivered to a deposition head (KUKA REIS MWO-I) by a 50 μm feeding fiber, connected to a 400 μm process fiber through a fiber-to-fiber coupler. The laser beam is collimated with a 129 mm lens, then focalized nearby the deposition region by means of a lens with 200 mm focal length. Adjusting the position of the collimating lens allows to change the spot diameter on the substrate from 0.7 mm to 3.5 mm. In the current work the collimator position was set for a 1.4 mm spot diameter.

Table 1. LMD setup parameters.

Process laser source	IPG YLS-3000
Laser power	400 W
Emission wavelength	1070 nm
Beam spot diameter	1.4 mm
Deposited material	AISI 316L powder
Reference SOD	12 mm
Process focal length	$f_1 = 200$ mm

The deposition head is mounted on a 6-axis anthropomorphic robot (ABB IRB 4600-45) and mounts a three-jet powder nozzle (FRAUNHOFER ILT 3-JET-SO16-S).

The metallic powder to be deposited is fed to the nozzle by a powder feeder (GTV TWIN PF 2/2-MF), using nitrogen both as vector gas and as nozzle shielding gas. The processed material is AISI 316L powder, with a powder size distribution between 45 μm to 90 μm (LPW). During the experiments the powder flow rate was fixed at 8.5 g/min. The substrate material is AISI 304 stainless steel with a 5 mm thickness. The reference SOD is set to 12 mm.
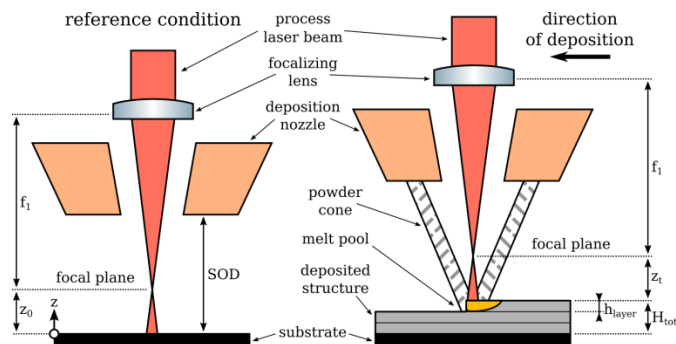

Fig. 1. Schematic section of the powder nozzle with the main dimensions and vertical coordinates related to the deposition height, both in the initial condition (left) and during the deposition (right).

2.2. Coaxial triangulation setup

The main dimensions related to the LMD setup are represented in Figure 1, while the parts of the optical setup are sketched in Figure 2. The light source used as probe for the triangulation measurement is a collimated laser diode module (THORLABS CPS532) emitting 4.5 mW of green light at 532 nm, with a circular beam shape of 3.5 mm diameter. The probe source is housed in a custom unit fixed sideways to the deposition head. The probe beam passes through a 50:50 non-polarizing beam-splitter cube (THORLABS BS004), which is used to superimpose on the same optical path the probe beam and the imaging system. Half of the probe intensity is then reflected by the cube and lost, half is transmitted toward the deposition head. A dichroic mirror, designed for transmitting the infrared radiation, deflects the probe beam by 90° with a reflectivity of about 72% at 532 nm. Such dichroic mirror allows to superimpose the probe and process beams along the common optical axis of the deposition head. Subsequently the collimated probe beam reaches the convergent lens with focal length $f_1 = 200$ mm which is used to focalize the process laser. Finally, the beam passes through the 6 mm diameter orifice of the deposition nozzle. The optical focal point stands approximately 3 mm out from the nozzle tip.

When the probe laser hits a target out from the nozzle it gets scattered around the incidence point. At the typical SOD values and in the hypothesis of isotropic scattering from a non-reflective surface, only about the 3% of the probe light intensity that gets scattered on the whole semi-spherical solid angle can go backwards to the deposition head trough the nozzle aperture. Such back-reflected radiation is collected and collimated by the f_1 lens, then deflected by the dichroic mirror to the triangulation unit. A shortpass wavelength filter (THORLABS FESH1000) with 1000 nm cutoff protects the components from the infrared light of the high-power process laser, which might come from the deposition area or from

parasitic reflections of the optical elements. The beam-splitter reflects half of the scattered light to the imaging arm, while half of the power is transmitted and lost.
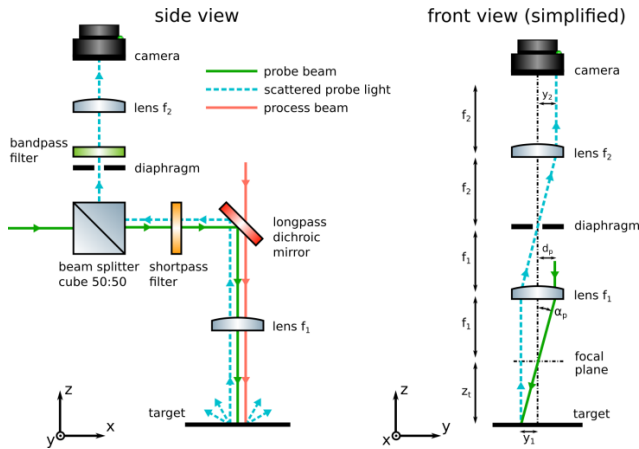

Fig. 2. Sketch of the optical setup used for the height monitoring. On the left, side view of the superimposed probe and process beams, with the imaging system used to detect the light scattered by the target. On the right, projected and simplified front view.

A second convergent lens with focal length $f_2 = 125$ mm is placed at distance $f_1 + f_2$ from the focalizing lens of the deposition head. This completes a telescope with an image magnification equal to

$$M = f_2/f_1 \simeq 0.63 \qquad (1)$$

on the CCD sensor of a monochrome camera (IDS UI-6230RE-M-GL) placed at distance f_2 from the imaging lens. The camera sensor has a total resolution of 0.8 MP and a pixel size of 4.65 μm. A 1 mm diameter diaphragm is placed in the focal point between the f_1 and f_2 lenses. This acts as spatial filter for the off-focus light beams, such as the back-reflections coming from the deposition head optical elements, which are not optimized for the visible wavelengths. At the diaphragm level a notch spectral filter (THORLABS FL05532-1) lets pass only the 532 nm wavelength with a FWHM of 1 nm, hence filtering the noise given by other light sources, such as the thermal emission coming from the melt pool or the ambient light. The use of both spectral and spatial filters allows to strongly enhance the signal-to-noise ratio for the weak signals given by the scattered probe light.

If the probe beam is perfectly aligned with the optical axis of the deposition head, hence hitting the dichroic mirror and the lens in their centers, it will be focused along the same optical path of the process beam. Conversely, if the probe beam is slightly displaced from the optical axis by a distance $d_p > 0$, it will be deflected by an angle $\alpha_p > 0$ relatively to the optical axis. Therefore, if the probe beam size is neglected and treated as a single optical ray, it will pass through the f_1 lens focal point with a deflection angle equal to

$$\alpha_p = \tan^{-1}\left(\frac{d_p}{f_1}\right). \qquad (2)$$

Such beam deflection introduces a linear dependence between the vertical distance z_t of the target from the focal plane and the coordinate y_1 of the probe spot in the horizontal plane related to the optical axis, thus

$$y_1 = \frac{d_p}{f_1} z_t. \qquad (3)$$

The probe spot is imaged on the camera sensor at different positions depending on z_t and α_p. Since the triangulation device is designed for a one-dimensional only measurement, the image position on the CCD sensor can be described by means of a single coordinate y_2 defined by the deflection plane of the probe beam:

$$y_2 = My_1 = \frac{f_2 d_p}{f_1^2} z_t. \qquad (4)$$

A higher off-axis displacement d_p reflects in a higher deflection angle α_p and in a better vertical sensibility. However, the design of the triangulation device must also take into account the requirement of independence of the height measurement on the direction of deposition. Therefore, the probe beam must be aligned in a quasi-coaxial way, i.e. with α_p small such that the probe beam keeps hitting the actual deposition area for a reasonable measurement interval of z_t. The typical width of the melt pool is of the order of 1 mm: this means that, for a vertical measurement range of ± 10 mm and a maximum displacement in the horizontal deposition plane of ± 0.5 mm, the beam misalignment must be $d_p \lesssim 10$ mm. In the current experimental conditions, the actual value of d_p is limited to about 8 mm by the clear aperture of the deposition head interface.

Table 2. Parameters of the triangulation setup.

Probe laser source	THORLABS CPS532
Laser power	4.5 mW
Emission wavelength	532 nm
Beam displacement	$d_p \simeq 5.6$ mm
Beam deflection angle	$\alpha_p \simeq 1.6°$
CCD pixel size	4.65 μm
Acquisition rate	98.4 Hz
Imaging focal length	$f_2 = 125$ mm

The camera acquisition is cropped to a region of 340×120 pixels. The sensor integration time is set to 10 ms with a framerate of 98.4 Hz. The acquired image sequence is analyzed with a PYTHON code as in the example of Figure 3. The intensity of each image frame is integrated along the short axis of the image, aligned such that the spot position along that direction is insensitive to z_t. A 1D-Gaussian is fitted to the integrated profile, allowing to extract the coordinate of the spot center. With such fitting procedure the centroid position can be determined with a resolution that, in principle, can go beyond the pixel resolution, hence being able to interpolate the y_2 coordinate on a sub-pixel scale.
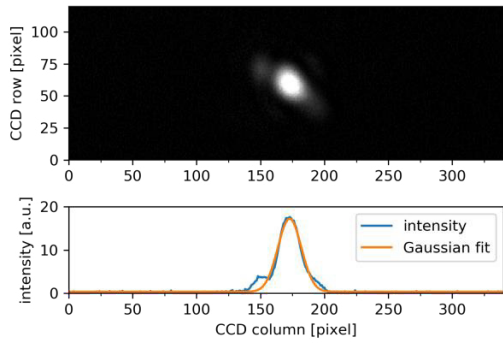
Fig. 3. Example of a frame acquired with the CCD camera, with the probe spot visible in the center. The column intensity is integrated in the lower plot and fitted to a Gaussian function in order to find the position of the spot centroid.

3. System calibration

The triangulation device has been calibrated by measuring y_2 for a number of known values of z_t in absence of the deposition process. This is accomplished with a motorized lab jack (THORLABS L490MZ/M) placed below the deposition head, which allows to control precisely the vertical coordinate of a dummy target with a 20 nm resolution and a 5 μm repeatability. The height of the target z_t has been varied relatively to the height z_0 corresponding to the reference SOD of 12 mm, from $z_0 - 10$ mm to $z_0 + 15$ mm.

The calibration curve is reported in Figure 4. The data are centered around $y_2 = 0$ and fitted to a linear function defined as

$$z_t - z_0 = a + by_2. \tag{5}$$

The proportionality factor was calculated as

$$b = (58.0 \pm 0.7) \text{ mm/mm} \tag{6}$$

from the linear regression, and it sets the sensibility in the height measurement. Consequently, the height increment corresponding to a single CCD pixel displacement equals to (0.270 ± 0.003) mm/pixel.
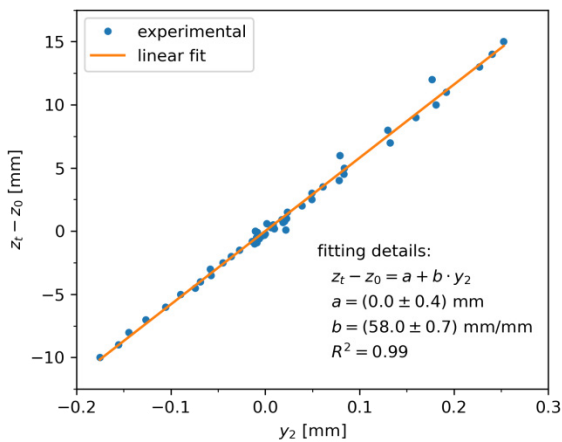

Fig. 4. Calibration curve for the triangulation device, with the relative height plotted as a function of the position of the probe spot centroid on the camera sensor.

4. Case study

In the 3-jet nozzle the powder is ejected by three orifices arranged with an angle of 120° between each other. The powder flow converges to the deposition zone generating the powder cone, which can introduce anisotropy according to the deposition direction. In order to quantify such phenomenon, the height monitoring device has been tested during the deposition of a multi-layer vertical wall. The wall is designed as a single straight track 150 mm long as sketched in Figure 5, deposited forward-and-backwards at the constant speed of 16 mm/s for a total of 42 layers. Starting from the initial SOD of 12 mm, the height of the deposition head is raised by $h_{robot} = 0.3$ mm at each deposited layer, i.e. the value of the deposition growth expected from preliminary tests.
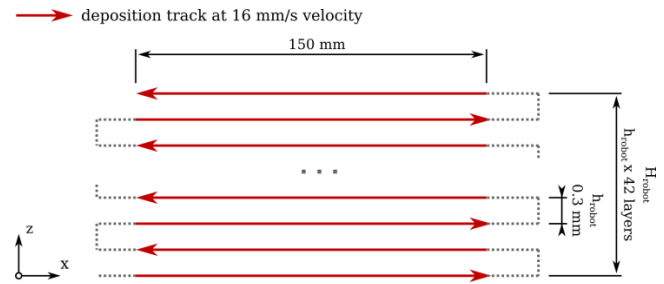

Fig. 5. Scheme of the deposition strategy for the vertical wall.

The measured relative height has been averaged for each deposited layer. By knowing the height set to the robot after a number of N_l layers, i.e.

$$H_{robot} = h_{robot} \cdot N_l, \tag{7}$$

it is possible to calculate the effective wall height as

$$H_{tot} = H_{robot} - (z_t - z_0). \tag{8}$$

The results are reported in Figure 6. The effective height of the final structure is also plotted for comparison. It can be observed that, layer by layer, the wall grows faster than the programmed height H_{robot}, with a final discrepancy of few millimetres. This suggests that the height increment h_{robot} underestimates the effective deposition growth h_{layer}. Another factor that can be observed from the experimental data is that a strong mismatch is present in the growth between odd (forward) and even (backwards) layers. This could be the signature of a difference in the deposition efficiency along the two opposite directions: such mismatch is probably caused by the anisotropic powder distribution coming from the 3-jet nozzle and, consequently, by a variable overlapping factor of the process laser beam on the deposition area. A quantitative knowledge and correction of such phenomena might enhance the deposition quality, in particular in the case of more complex structures.
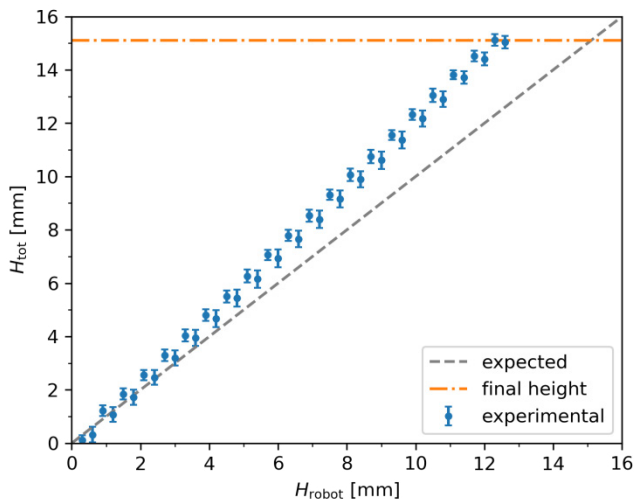
Fig. 6. Average wall height measured for each layer, plotted as a function of the height programmed to the robot. The error bars refer to standard deviation within the layer. The departure from the expected behaviour highlights a mismatch between programmed height increment and deposition growth. The final wall height is measured with a digital calliper and reported for comparison.

5. Conclusions

In current paper a device for the deposition height monitoring has been presented, based on the triangulation principle and implemented with an innovative design on a LMD setup. The working principle of the device has been demonstrated during the deposition of a multi-layer wall. The coaxial configuration allows for high flexibility in terms of deposition strategy and direction. This may represent a simple, non-intrusive, and low-cost solution for the real-time monitoring of the deposition growth, with the aim of providing a feedback signal for controlling actively the process parameters, hence improving the deposition quality and the geometry regularity in the final structure.

Acknowledgements

References

[1] Frazier WE. Metal Additive Manufacturing: A Review. Journal of Materials Engineering and Performance 2014;23:1917–28.
[2] Pinkerton AJ, Li L. The significance of deposition point standoff variations in multiple-layer coaxial laser cladding (coaxial cladding standoff effects). International Journal of Machine Tools and Manufacture 2004;44:573–84.
[3] Zhu G, Li D, Zhang A, Pi G, Tang Y. The influence of standoff variations on the forming accuracy in laser direct metal deposition. Rapid Prototyping Journal 2011;17:98–106.
[4] Everton SK, Hirsch M, Stravroulakis P, Leach RK, Clare AT. Review of in-situ process monitoring and in-situ metrology for metal additive manufacturing. Materials & Design 2016;95:431–45.
[5] Kim H, Lin Y, Tseng T-LB. A review on quality control in additive manufacturing. Rapid Prototyping Journal 2018;24:645–69.
[6] Heralić A, Christiansson A-K, Lennartson B. Height control of laser metal-wire deposition based on iterative learning control and 3D scanning. Optics and Lasers in Engineering 2012;50:1230–41.
[7] Denlinger ER, Heigel JC, Michaleris P, Palmer TA. Effect of inter-layer dwell time on distortion and residual stress in additive manufacturing of titanium and nickel alloys. Journal of Materials Processing Technology 2015;215:123–31.
[8] Heigel JC, Michaleris P, Palmer TA. In situ monitoring and characterization of distortion during laser cladding of Inconel® 625. Journal of Materials Processing Technology 2015;220:135–45.
[9] Segerstark A, Andersson J, Svensson L-E. Investigation of laser metal deposited Alloy 718 onto an EN 1.4401 stainless steel substrate. Optics & Laser Technology 2017;97:144–53.
[10] Tang L, Landers RG. Layer-to-Layer Height Control for Laser Metal Deposition Process. Journal of Manufacturing Science and Engineering 2011;133:021009.
[11] Song L, Bagavath-Singh V, Dutta B, Mazumder J. Control of melt pool temperature and deposition height during direct metal deposition process. The International Journal of Advanced Manufacturing Technology 2012;58:247–56.
[12] Biegler M, Graf B, Rethmeier M. In-situ distortions in LMD additive manufacturing walls can be measured with digital image correlation and predicted using numerical simulations. Additive Manufacturing 2018;20:101–10.